

# Supplementary Information

## Replacing Metals with Oxides in Metal-Assisted Chemical Etching Enables Direct Fabrication of Silicon Nanowires by Solution Processing

*Maxime Gayrard,<sup>1</sup> Justine Voronkoff,<sup>1</sup> Cédric Boissière,<sup>1</sup> David Montero,<sup>2</sup> Laurence Rozes,<sup>1</sup> Andrea Cattoni,<sup>3</sup> Jennifer Peron,<sup>4</sup> Marco Faustini<sup>1\*</sup>*

*1 Sorbonne Université, CNRS, Collège de France, Laboratoire Chimie de la Matière Condensée de Paris (LCMCP), F-75005 Paris, France*

*2 Sorbonne Université, Institut des Matériaux de Paris Centre (IMPC FR 2482), UFR de Chimie Campus Jussieu, 75252 Paris, France*

*3 Centre de Nanosciences et de Nanotechnologies (C2N), CNRS UMR 9001, Université Paris-Saclay, Palaiseau, France.*

*4 Université de Paris, ITODYS, CNRS, UMR 7086, 15 rue J-A de Baïf, F-75013 Paris, France*

*e-mail: marco.faustini@sorbonne.universite.fr*

## Materials and Methods

### a) Chemicals

Ruthenium(III) chloride hydrate ( $\text{RhCl}_3 \cdot x\text{H}_2\text{O}$ , Sigma Aldrich), Iridium(III) chloride hydrate ( $\text{IrCl}_3 \cdot x\text{H}_2\text{O}$ , Alfa Aesar), poly(butadiene)-poly(ethylene oxide) (PB-PEO, Mn 5600 g.mol<sup>-1</sup> PB and 10000 g.mol<sup>-1</sup> PEO, from Polymer Source). 6 inch -diameter p-type (100) Si wafer with a resistivity of 1-10 ohm-cm was purchased from Siltronix Silicon Technologies

### b) Soft-Nanoimprinting Lithography

#### *Master and PDMS-based stamp fabrication*

The silicon master mold was fabricated by electron beam lithography at 100 KeV (Vistec 5000+) and reactive ion etching. An A7 PMMA positive-tone resist (495PMMA A Resists, solids: 7% in Anisole) was spin-coated on a 2-inch Si(100) wafer and baked for 45 min at 160 °C. The sample was exposed at 10 nA with a dose of 1300  $\mu\text{C}/\text{cm}^2$ , developed for 45 sec in a solution of Methyl-isobutyl-ketone (MIBK) and Isopropanol (mixture 1:3), rinsed in Isopropanol and gently dried with pure nitrogen gas. The pattern was transferred by reactive ion etching using a  $\text{SF}_6/\text{CHF}_3$  gas mixture.

The anti-sticking treatment was performed using 1H,1H,2H,2H-Perfluorooctyltriethoxysilane (POTS) by chemical vapor deposition method. A sealed glass Petri dish containing the Silicon master and several drops of POTS was heated in an oven at about 120 °C for 1 h to enable the reaction between the OH groups on the Si substrate surfaces and the POTS and then maintained at about 150 °C for 2 h to remove the unreacted POTS molecules.<sup>1</sup>

A bi-layer hard-PDMS/PDMS stamp was then replicated first by spin-coating a thin hard-PDMS layer on the silicon master and secondly by casting a mixture of commercial available (RTV615 from GE) two components solution (1:10) on top. The bi-layer hard-PDMS/PDMS stamp was degassed and soft-baked at 60 °C for 48 h. Finally, after being peeled off from the silicon master, the bi-layer stamp was treated with trichloromethylsilane TMCS.<sup>2</sup>

#### *Imprinting*

0.244 g of metal salt precursor was dissolved in EtOH/H<sub>2</sub>O (7/1, w/w) solution. PDMS mold was placed under vacuum for 30 min. The silicon wafer was cleaned with ethanol solution and oxygen plasma. The silicon substrate was coated with iridium or ruthenium solution via dip-coating. Dip-coating was performed in a closed chamber with controlled atmosphere at relative humidity < 10 % and room temperature. The process consisted in (i) dipping the substrate into the tank (ii) letting it immersed for three seconds, (iii) withdrawing at speed of 10 mm/s (iv) letting it in the close chamber for 1 minutes to allow complete evaporation of the solvent. Just after the deposition, the PDMS mold was applied on silicon surface and it was placed in oven at 130 °C for 5 min. The PDMS mold was then removed and the film was calcined at 300 °C under air.

### c) Block-copolymers Lithography

0.020g of PB-PEO was dissolved in a EtOH/H<sub>2</sub>O (7/1, w/w) solution. To induce complete dissolution of the block-copolymer, the solution was warmed at 70°C for 30 minutes. After cooling, 0.122 g of salt metal precursor was added to the solution. The silicon wafer was cleaned with ethanol solution and oxygen plasma. The substrate was coated with iridium or ruthenium solution via dip-coating performed in a controlled atmosphere at relative humidity < 10 % and room temperature and with a slow withdrawal speed of 0.7 mm/s allowing formation of a monolayer of micelles.

#### d) Characterization

RuO<sub>2</sub> film was analyzed by X-Ray diffraction (XRD), XRD measurements were carried out using a Panalytical X'pert pro diffractometer equipped with a Co anode ( $\lambda K\alpha = 1.79031 \text{ \AA}$ ) and a multichannel X'celerator detector. The XRD pattern was indexed to the ICSD card 03-065-2824 for RuO<sub>2</sub>. XPS spectra were recorded using a K-Alpha+ spectrometer from Thermofisher Scientific, fitted with a microfocused, monochromatic Al K <sub>$\alpha$</sub>  X-ray source ( $h\nu = 1486.6 \text{ eV}$ ; spot size = 400 micrometers). The pass energy was set at 150 and 40 eV for the survey and the narrow regions, respectively. Spectral calibration was determined by setting the main C1s (C-C, C-H) component at 285 eV.

The optical properties of the films were characterized using spectroscopic ellipsometry (M2000, J.A. Woollam) with a thermal or environmental chamber. SEM imaging was performed on a SU-70 Hitachi FESEM. Voltage acceleration setup was 5 kV and usually upper detector was used for secondary electron acquisition except in fig S2 where M is noted, which stands for upper and lower detector at the same time. The surface morphology of the films was studied using an AFM Nanosurf C3000 equipment. Height images and profiles were recorded on 10  $\mu\text{m}^2$  area

#### e) Etching

The etching solution was prepared with 0.326g H<sub>2</sub>O<sub>2</sub> (50%); 31,6 g H<sub>2</sub>O and 8,3 ml HF (48%). The samples were immersed in the etching solution at different times. After etching, the sample was cleaned with ethanol solution.

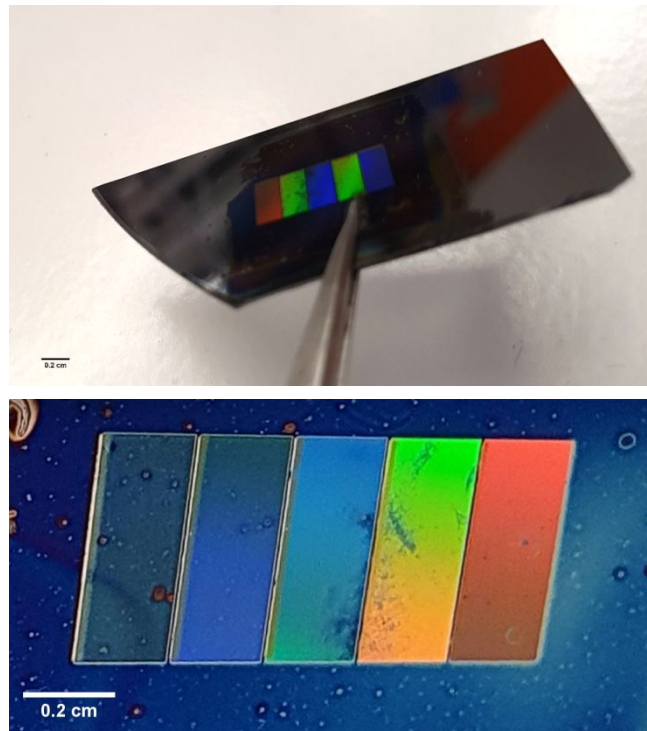


**Figure S1** Photos of a patterned sample of 4 cm<sup>2</sup> exhibiting areas with different iridescent colors characteristic of diffraction gratings with periodicities ranging from 400 to 1000 nm.

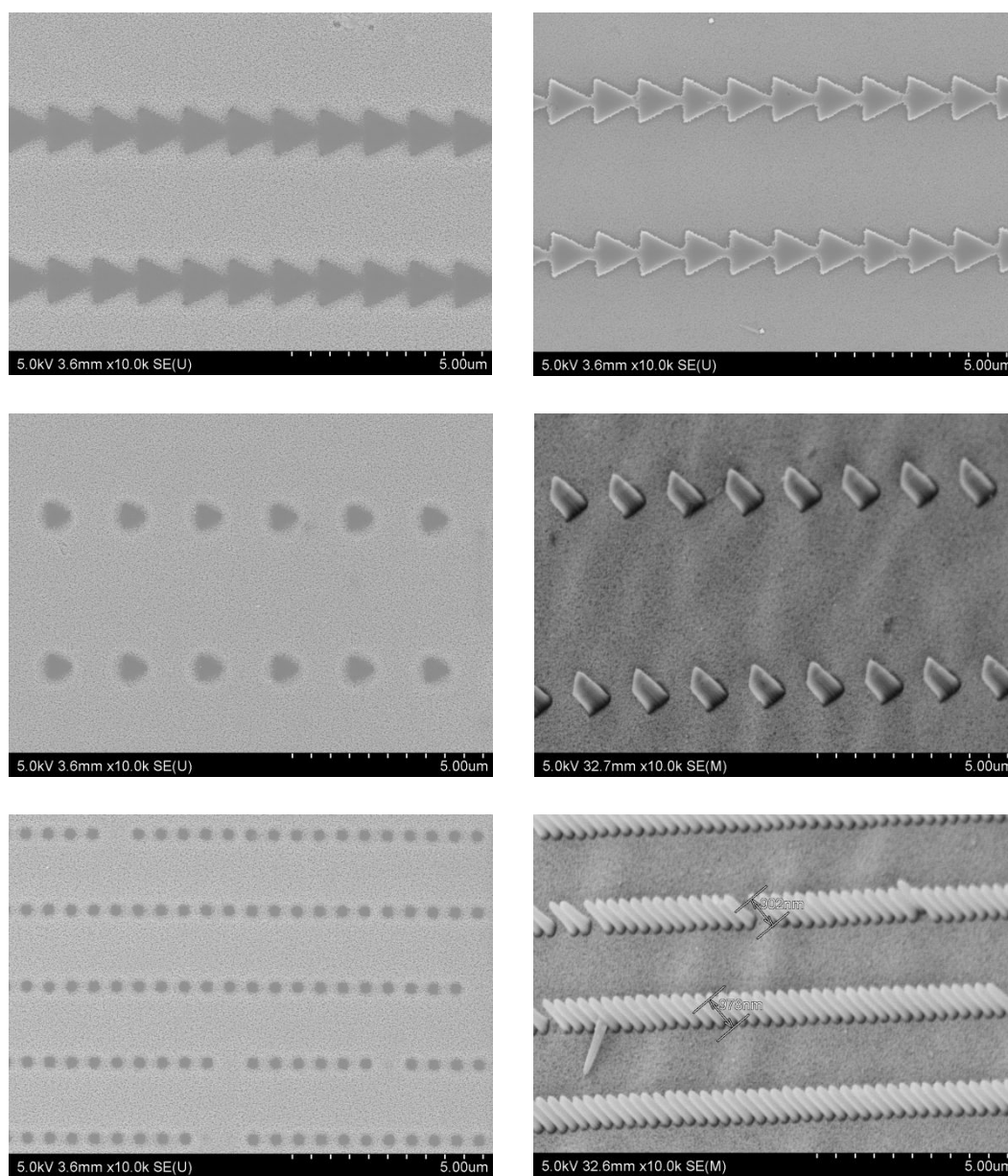
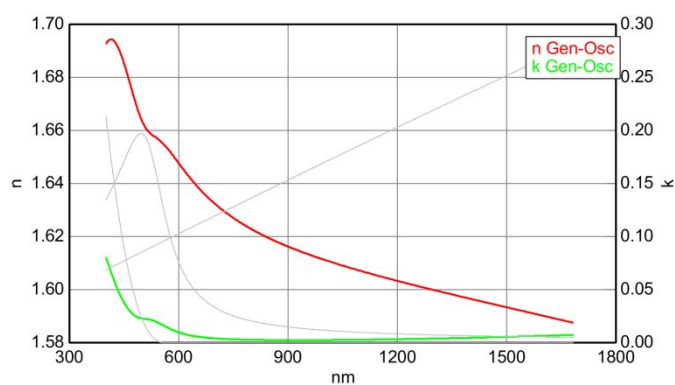
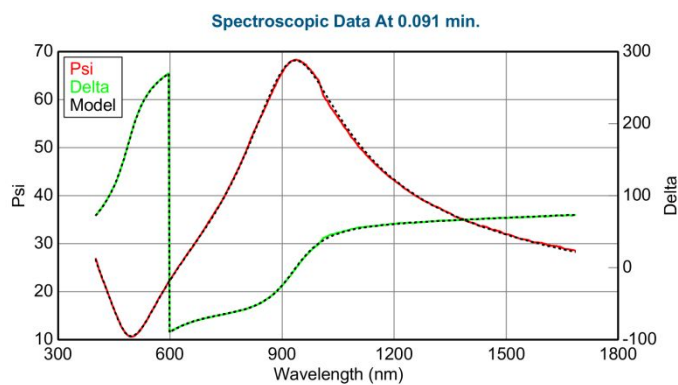


**Figure S2** Residual layer-free RuO<sub>2</sub> masks (left) obtained after soft-nanoimprinting lithography; silicon nanostructures after OACE (right).

### Ellipsometric model for Ru-based film at room temperature



### Ellipsometric fit of the film at room temperature



### Ellipsometric fit of the film at 195°C

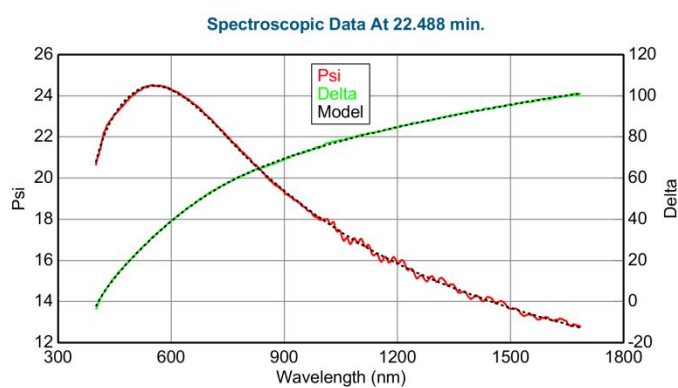
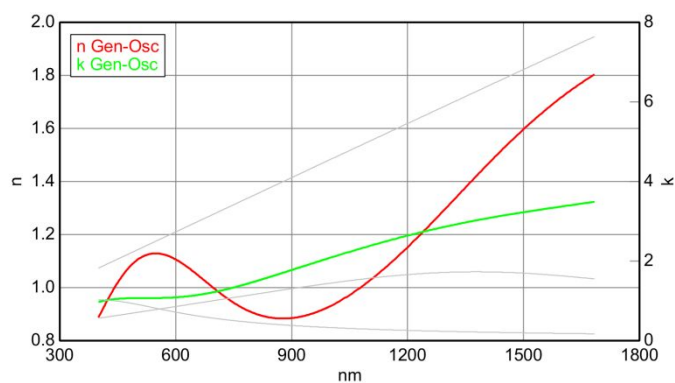
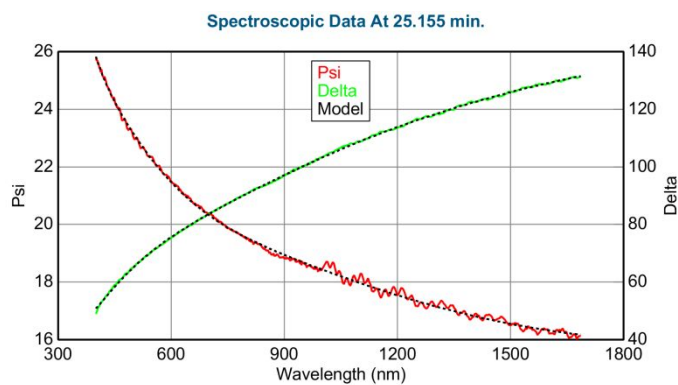


**Figure S3** Ellipsometric model for Ru-based films below 200°C

*Ellipsometric model for Ru-based film at 300°C*



*Ellipsometric fit of the film at 210 temperature*



*Ellipsometric fit of the film at 300°C*

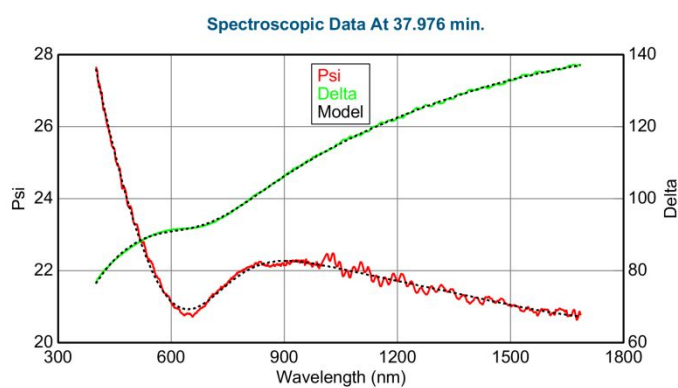
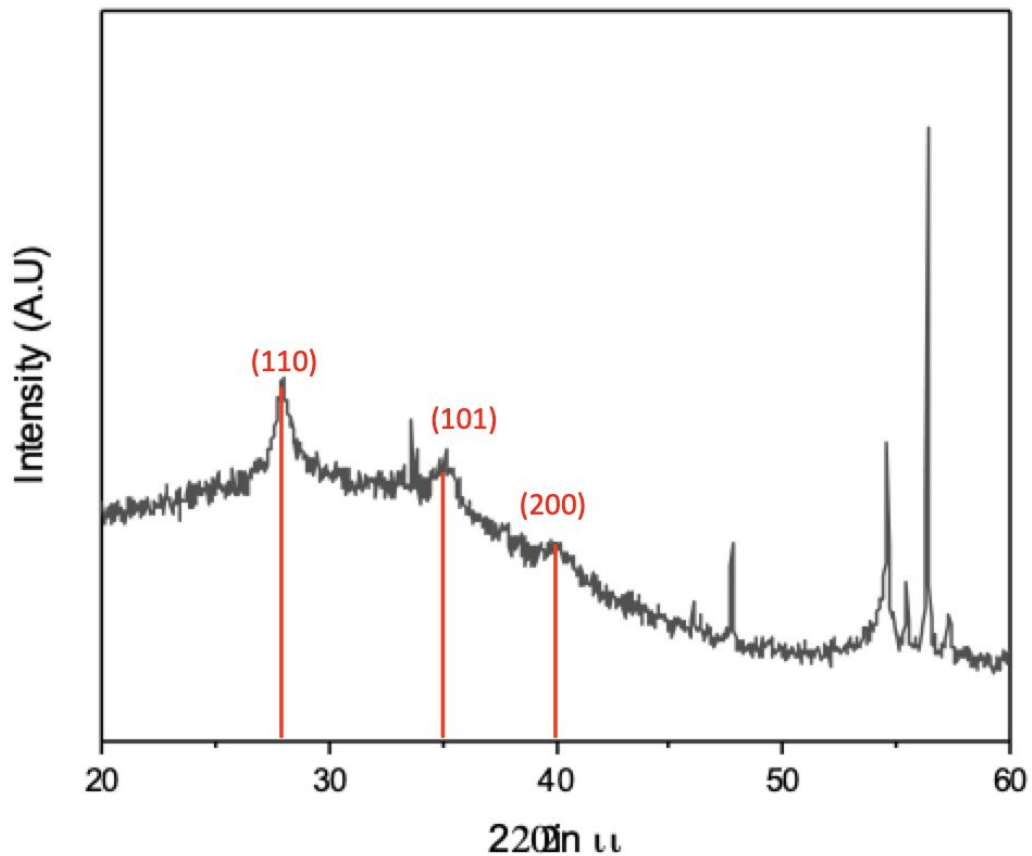


**Figure S4** Ellipsometric model for Ru-based films above 200°C



The crystallite size was determined by Scherrer equation :

$$\tau = \frac{k\lambda}{\beta \cos(\theta)}$$

where:

$\tau$  : size of crystallite

k: shape factor 0,89

$\lambda$  : Wavelength of Cu ( $\lambda=1,54 \text{ \AA}$ )

$\theta$  : glancing angle (rad)

$\beta$  : Full width at half maximum (FWHM)

The average crystal size was calculated by considering the peak 110 with

$2\theta$  : 27,97

$\beta$  : 0,739

**Figure S5** XRD of the RuO<sub>2</sub> film treated at 300°C and analysis of the crystal size



## Ellipsometric Porosimetry

The measurement is performed by placing the film into a closed chamber in which a vapor flux was injected to control the relative vapor pressure ( $P/P_0$ ). The evolution of the refractive index at 330nm as function of the experimental time is shown hereafter. We selected the values of refractive index at 330nm because in the UV region (330 nm) the film is less absorbing than in the visible or near IR range, simplifying the following quantitative analysis.

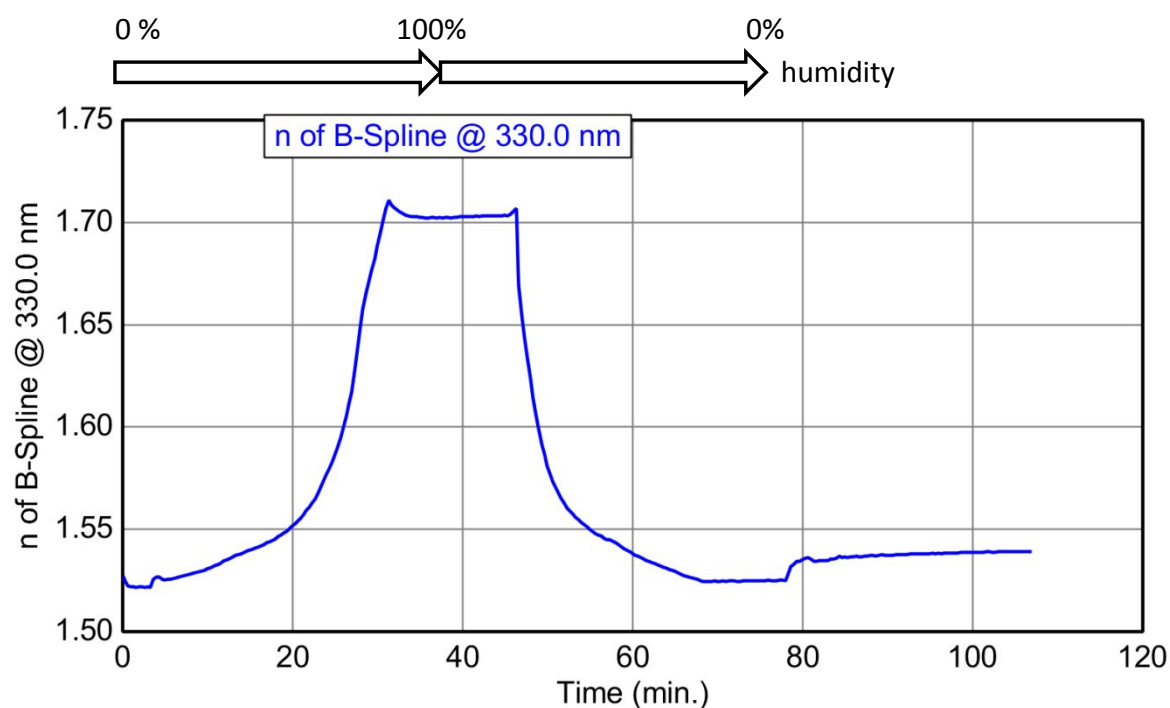


**Figure S6** Ellipsometric porosimetry: evolution of the refractive index of RuO<sub>2</sub> film as function of the time performed in a closed chamber in which humidity is increased and then decreased.

## Porosity analysis

From the data of refractive index, the water uptake % vol could be determined by using Bruggemann effective medium approximation (BEMA) model with three components:<sup>3</sup>

$$f_{air} \frac{\epsilon_{air} - \epsilon}{\epsilon_{air} + 2\epsilon} + f_{wall} \frac{\epsilon_{wall} - \epsilon}{\epsilon_{wall} + 2\epsilon} + f_{water} \frac{\epsilon_{water} - \epsilon}{\epsilon_{water} + 2\epsilon} = 0 \quad (1)$$

in which  $f_{air}$ ,  $f_{water}$  and  $f_{wall}$  and  $\epsilon_{air}$ ,  $\epsilon_{water}$  and  $\epsilon_{wall}$  represent the volumetric fraction and dielectric constant of air, water and of the solid wall that is composed by RuO<sub>2</sub> nanoparticle wall respectively. The value of  $\epsilon_{wall}$  and  $f_{wall}$  were determined by combining the ellipsometric data of the "empty" film (low  $P/P_0$ ) and "water filled" film (high  $P/P_0$ ) by considering that that  $f_{air}$  at low  $P/P_0$  is equal to the  $f_{water}$  at high  $P/P_0$ . The total porous volume -  $(1-f_{wall})$  % could be quantified to be 45%.

The porosity is characterized by a narrow adsorption-desorption hysteresis suggesting that pores are highly interconnected through large pore windows. The pore size distributions of porous films were determined from the adsorption curve, using the Kelvin equation:

$$\ln \frac{P}{P_0} = - \frac{\gamma V_l \cos \theta}{r_p RT} \quad (2)$$

where  $(P/P_0)$  is the water relative pressure and  $r_p$ ,  $\gamma$ ,  $V_l$ ,  $\theta$ ,  $R$ , and  $T$  are the Kelvin pore radius, the surface tension, the molar volume of liquid, the contact angle, the gas constant and the temperature, respectively.<sup>4</sup> The pore size distribution is reported in Figure S7 indicating a broad size distribution with average pore dimension of 12 nm in agreement with the SEM observations.

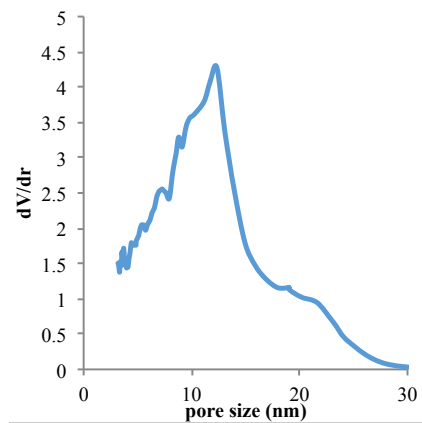


**Figure S7** Pore size distribution in the RuO<sub>2</sub> films obtained by ellipsometric porosimetry



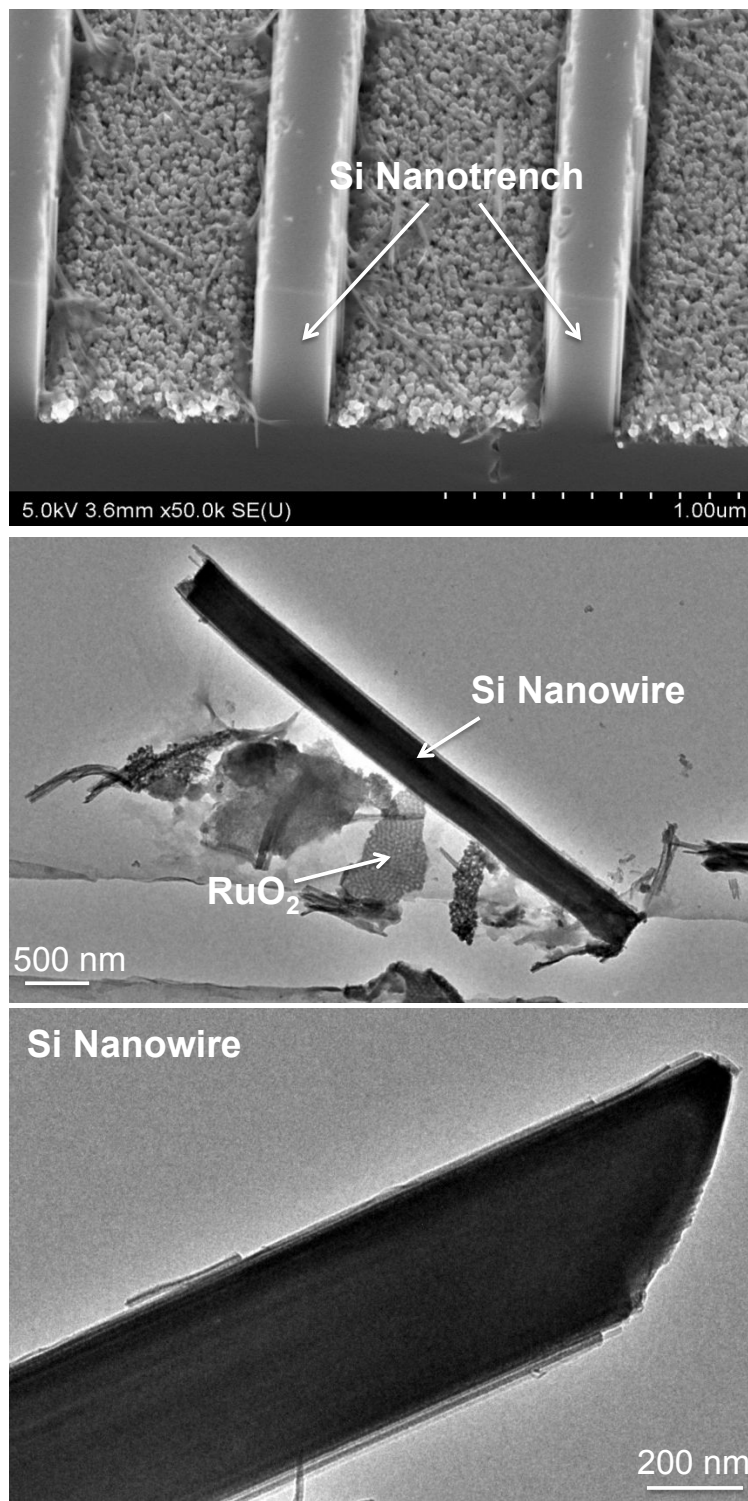


**Figure S8: (top)** SEM of silicon nanotrench arrays and **(middle and bottom)** TEM micrographs of a single Si nanowire at different magnifications

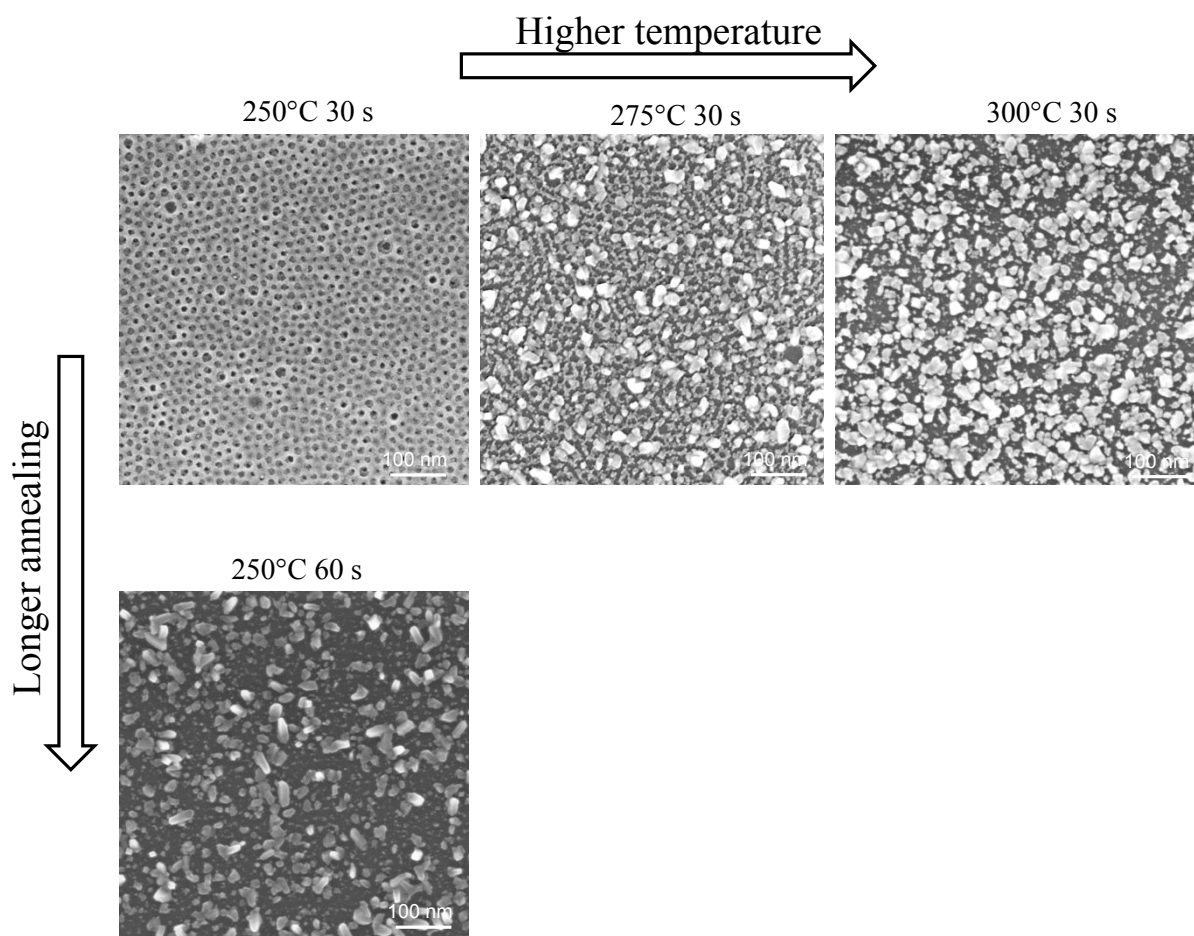


**Figure S9** SEM micrographs of the block-copolymer templated  $\text{RuO}_2$  film treated at different temperatures and times

## Etching rate

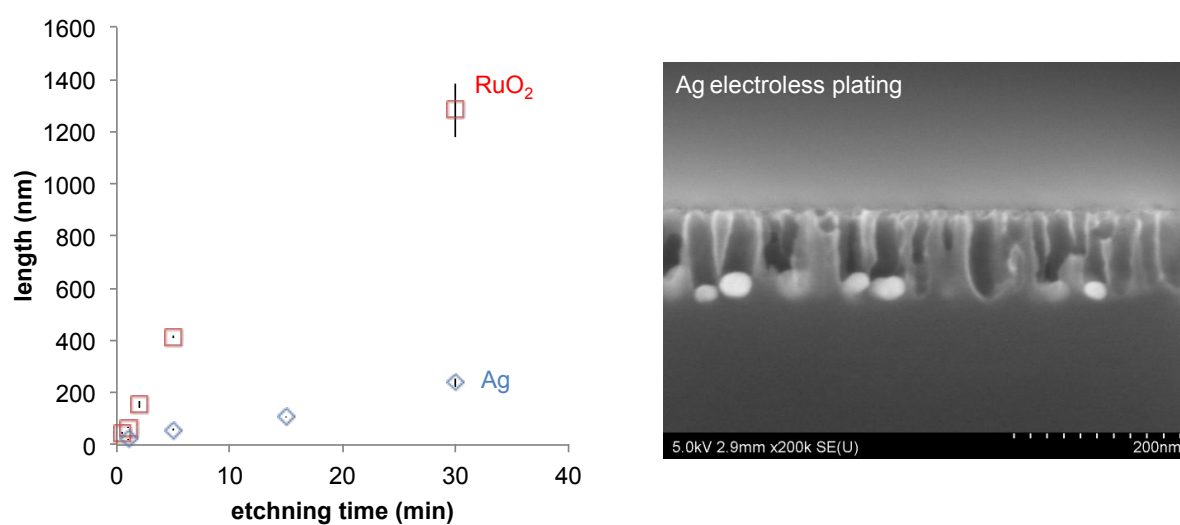


**Figure S10** (right) Evolution of the nanowires length obtained from block-copolymer templated RuO<sub>2</sub> masks and from Ag electroless plating as function of the etching time (left) SEM micrograph of the Ag nanoparticles etched for 15 minutes

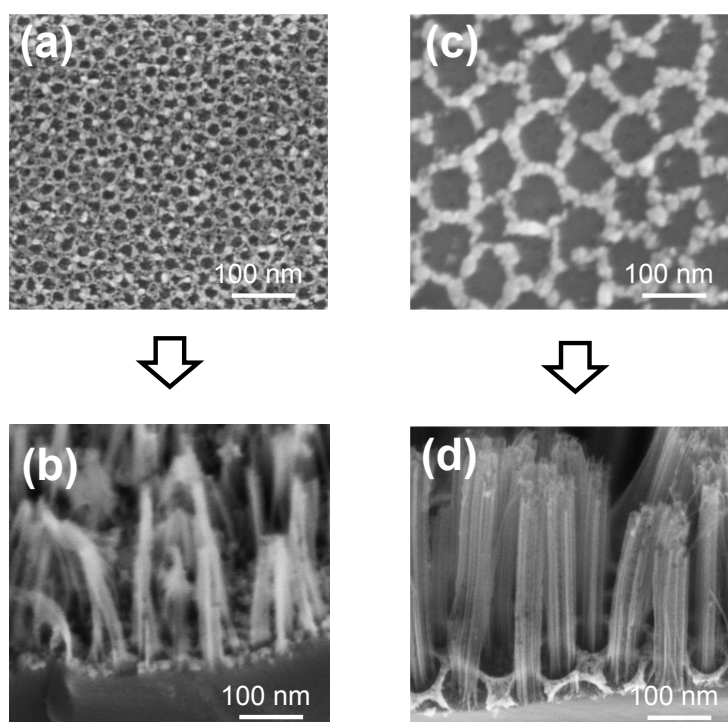
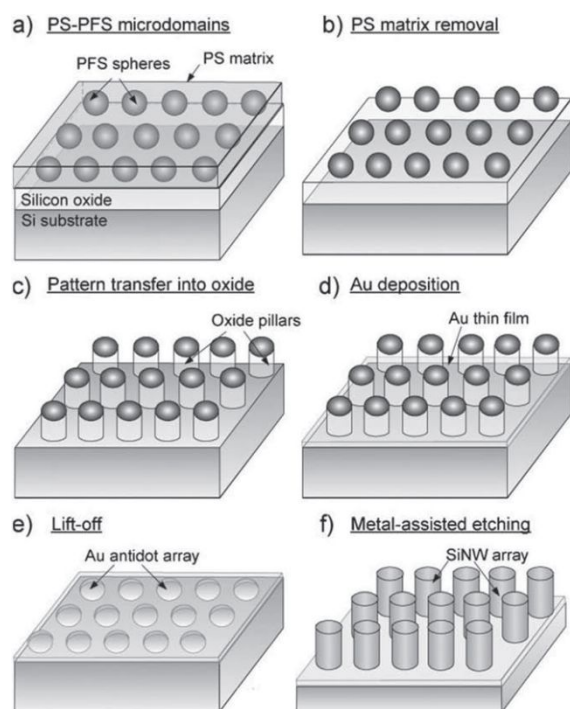


**Figure S11** SEM micrographs: (a) and (c) nanoporous IrO<sub>x</sub> films obtained from small and large block-copolymer template respectively; (b) and (d) after 5 minutes etching respectively

## Block-copolymer lithography + MACE



## Block-copolymer lithography + OACE

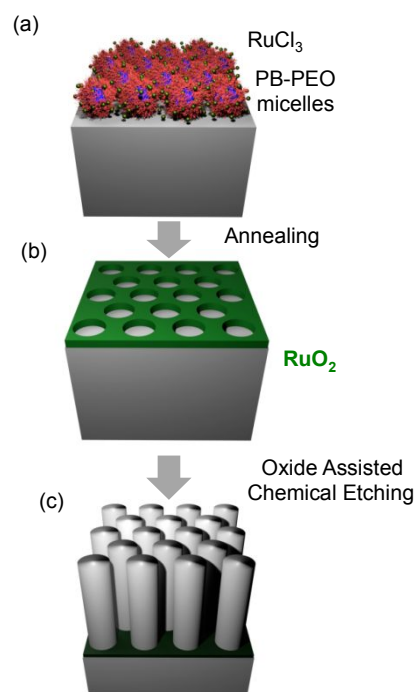


**Figure S12** Comparison between the two methods to obtain sub 20 nm silicon nanowires by MACE<sup>5</sup> (left) and by OACE (right, this work).

- 1 Wang, L., Wei, J. & Su, Z. Fabrication of Surfaces with Extremely High Contact Angle Hysteresis from Polyelectrolyte Multilayer. *Langmuir* **27**, 15299-15304, doi:10.1021/la2039448 (2011).
- 2 Cattoni, A., Cambril, E., Decanini, D., Faini, G. & Haghiri-Gosnet, A. M. Soft UV-NIL at 20 nm scale using flexible bi-layer stamp casted on HSQ master mold. *Microelectronic Engineering* **87**, 1015-1018, doi:<http://dx.doi.org/10.1016/j.mee.2009.11.106> (2010).
- 3 Li, R., Faustini, M., Boissière, C. d. & Grosso, D. Water capillary condensation effect on the photocatalytic activity of porous TiO<sub>2</sub> in air. *The Journal of Physical Chemistry C* **118**, 17710-17716 (2014).
- 4 Li, R., Boudot, M., Boissière, C., Grosso, D. & Faustini, M. Suppressing structural colors of photocatalytic optical coatings on glass: the critical role of SiO<sub>2</sub>. *ACS Applied Materials & Interfaces* **9**, 14093-14102 (2017).
- 5 Chang, S. W., Chuang, V. P., Boles, S. T., Ross, C. A. & Thompson, C. V. Densely packed arrays of ultra - high - aspect - ratio silicon nanowires fabricated using block - copolymer lithography and metal - assisted etching. *Advanced functional materials* **19**, 2495-2500 (2009).



